Journal of Agricultural Science; Vol. 11, No. 17; 2019
ISSN 1916-9752 E-ISSN 1916-9760
Published by Canadian Center of Science and Education

Influence of Soil on the Traction Performance of a 65 kW MFWD Tractor

A. Battiato[1,2] & E. Diserens[1]

[1] Agroscope, Institute for Sustainability Sciences, Ettenhausen, Switzerland

[2] Department of Land, Environment, Agriculture and Forestry, University of Padua, Legnaro, Padua, Italy

Correspondence: A. Battiato, Agroscope, Institute for Sustainability Sciences, CH-8356 Ettenhausen, Switzerland. E-mail: andreas.battiato@gmail.com

Received: June 1, 2019 Accepted: September 3, 2019 Online Published: October 15, 2019

doi:10.5539/jas.v11n17p11 URL: https://doi.org/10.5539/jas.v11n17p11

The research is financed by Swiss Federal Office for the Environment FOEN and Michelin.

Abstract

This study aimed to investigate the influence of the mechanical behaviour of the soil surface on the traction performance and the fuel consumption of an agricultural tractor, both in qualitative and in quantitative terms, in order to increase the consciousness about the major role of the soil mechanical response in the optimisation of the energy aspects involved in the traction developed by a tractor and promote the development of new strategies to reduce costs of tillage management and improve agricultural sustainability. The traction performance of a 65 kW MFWD tractor at tyre pressures of 60 and 160 kPa was compared on four Swiss agricultural soils: a clay with corn stubbles, a clay loam with wheat stubbles, a silty loam and a loamy sand both with corn stubbles. Tests performed with a bevameter pointed out noticeable differences in the mechanical behaviour of the soils. According to such differences, the drawbar pull on the four soils was significantly disparate with differences in maximal values of about 16% at a tyre pressure of 60 kPa and up to 37% at a tyre pressure of 160 kPa. Simulations with a semi-empirical tractor-soil interaction model also showed dissimilarities in traction coefficient, motion resistance, and traction efficiency. Measurements of the fuel consumption pointed out the presence of a narrow slip range where the specific fuel consumption SFC is minimised. This range doesn't vary significantly among the considered soils as well as with the tyre pressure and doesn't differ very much from the range where the power delivery efficiency is maximised. The SFC differed for almost 20% among the considered soils at a tyre pressure of 60 kPa and for ca. 10% at a tyre pressure of 160 kPa. The increase in tyre pressure from 60 to 160 kPa produced an increment in SFC up to 16%. The results of this study clearly pointed out how the traction performance is a characteristic of the tractor-soil system and not of the tractor only, therefore, a proper knowledge of the soil mechanical behaviour should aid in developing strategies oriented towards reducing fossil fuel consumption.

Keywords: terramechanics, MFWD tractor, soil strength, soil-tyre interaction

1. Introduction

Organic matter decrease, erosion, compaction, pollution, acidification and salinisation are identified as the most important threats affecting agricultural soils. Moreover, it is recognised how soil organic matter suffers from climate change (Oenema, Heinen, Peipei, Rietra, & Hessel, 2017) and fossil fuel consumption, affecting the charge of greenhouse gases, also influences soil fertility in the long run.

Many national and international research projects are currently focusing on the above aspects in order to develop and promote new strategies oriented towards improving agricultural sustainability. In this context, also the optimisation of the interaction between soil and agricultural vehicles is recognised as one of the major future challenges, as it is demonstrated how such aspect might easily turn out in a substantial decrease in fuel consumption and soil compaction (Battiato, Diserens, & Sartori 2014; Battiato, Alaoui, & Diserens, 2015; Battiato & Diserens, 2017). Within this framework, it is of certain interest to analyse and simulate the role of the soil in conditioning the traction performance, with particular regard to the fuel consumption, of an agricultural tractor.

The major role of the soil mechanical behaviour in controlling the traction performance of a vehicle in off-road locomotion was pointed out from the origins of Terramechanics (Bekker, 1956, 1960; Wong, 1967; Wong & Reece, 1967, parts 1 and 2).

Parameters describing the soil mechanical behaviour are present in the empirical, the semi-empirical, and the analytical methods used for analysing the tyre-soil interaction and predicting the trafficability of a terrain or the traction performance of an off-road vehicle.

In the context of the semi-empirical methods of tyre-soil interaction, like the one considered in this work, a thorough description of the mechanical tests with the bevameter was presented by Bekker (1956, 1960). An improved procedure to derive the soil mechanical parameters on the basis of the Bevameter compression and shear tests was proposed by Wong (1980).

The major attention to a proper mechanical characterisation of the terrain for predicting trafficability and traction performance is testified by many works (Wills, 1963; Wong, Garber, Radforth, & Dowell, 1979; Wong, Radforth, & Preston-Thomas, 1982; Wong & Preston-Thomas, 1983). Upadhyaya and Wulfsohn (1993) presented an instrumented device to obtain the soil parameters related to traction. More recently, Garciano, Upadhyaya, and Jones (2010) introduced an instrumented portable device that measures soil parameters useful in predicting tractive ability of off-road vehicles.

An analysis and quantitative evaluation of the effect of soil conditions on tractive performance of off-road wheeled and tracked vehicles was presented by Lyasko (2010). He concluded that in order to accurately calculate the tractive performance of a vehicle in a given soil condition, soil properties and parameters and their changes as functions of soil moisture content and density should be taken into account.

In spite of the recognised main role of the mechanical reaction of soil in controlling the traction performance of a tractor, only few examples of quantitative assessment of such a role have been presented so far (Schreiber & Kutzbach, 2008; Lyasko, 2010; Pentoś & Pieczarka, 2017).

A major interest focused on the possibility to improve the traction performance of a tractor by optimizing its configuration in terms of tyre inflation pressure, number of drive wheels and load acting on the wheels (Burt Bailey, Patterson, & Taylor, 1979; Burt & Bailey, 1982; Charles, 1984; Turner, 1993; Zoz & Grisso, 2003; Damanauskas, Janulevičius, & Pupinis, 2015; Battiato & Diserens, 2017). However, this aspect can't disregard the nature of the soil on which the tractor moves as well as the soil condition and the presence of vegetation, particularly post-harvest stubble. All these factors, in fact, affect the mechanical reaction of the soil and, as a consequence, the traction performance of the tractor which depends on the efficiency of the mechanical interaction between the soil and the traction system (wheels or tracks). A proper approach to the optimization of the traction performance of tractors should, therefore, regard the whole system of interaction tractor-soil, also considering the role of the vegetation cover (Battiato & Diserens, 2013, 2017).

In this context, this work aimed to assess the influence of the mechanical behaviour of the soil surface on the traction performance and the fuel consumption of a 65 kW MFWD agricultural tractor, both in qualitative and in quantitative terms, and simulate the above influence with a semi-empirical tractor-soil interaction model.

2. Material and Methods

2.1 Testing Locations

Three sites in north-eastern Switzerland and one site in north-west were chosen as testing locations. These locations presented very differentiated soil textures and conditions as reported in Table 1.

2.2 Soil Properties and Soil Tests

Topsoil properties of the four locations, presented in Table 1, were determined as described by Battiato and Diserens (2017).

A description of the bevameter used for the mechanical characterisation of the soil was reported by Diserens and Steinmann (2003), and recently by Battiato and Diserens (2017). Penetration and shear tests were performed as described by Battiato and Diserens (2013) and results were elaborated according to Wong (1980). In order to take into account the multi-pass effect, the mechanical tests were performed before tractor passage (first load) as well as on the rut left by the passage of the front wheel (second load). Only in the clay soil the compaction due to the passage of the front wheel altered the soil reaction in vertical plate penetration tests remarkably.

In Table 1, parameters $K_{c,f}$, $K_{\varphi,f}$ and n_f describe the interaction between soil and front wheel, whereas parameters $K_{c,r}$, $K_{\varphi,r}$ and n_r the interaction between soil and rear wheel. Parameters c, φ and k from horizontal plate shear deformation tests did not change appreciably due to the passage of the front wheel (Table 1).

Table 1. Physical and mechanical parameters of topsoil in the four locations considered

Soil property 0-0.10 m depth	C*	CL	SL	LS
Site	Tänikon	Tänikon	Frauenfeld	Witzwil
Latitude	47°28′52″N	47°29′0″N	47°34′32″N	46°59′30″N
Longitude	8°54′14″E	8°54′44″E	8°52′20″E	7°03′24″E
Sand [%]	20	31	20	84
Silt [%]	32	34	53	10
Clay [%]	48	35	27	6
Texture (USDA classification)	clay	clay loam	silty loam	loamy sand
Cover	corn stubble	wheat stubble	corn stubble	corn stubble
Volumetric water content θ [%]	27.0	28.4	40.2	15.2
Soil water potential [kPa]	6.11	9.45	1.27	57.40
Cohesive modulus of deformation (front) $K_{c,f}$ [kN/m$^{(n+1)}$]	2354.1	4554.8	298.2	1208.2
Frictional modulus of deformation (front) $K_{\varphi,f}$ [kN/m$^{(n+2)}$]	-4130.0	-3036.5	479.0	-805.5
Exponent of deformation (front) n_f	1.01	0.90	0.77	0.81
Cohesive modulus of deformation (rear) $K_{c,r}$ [kN/m$^{(n+1)}$]	2168.9	4554.8	298.2	1208.2
Frictional modulus of deformation (rear) $K_{\varphi,r}$ [kN/m$^{(n+2)}$]	-3498.3	-3036.5	479.0	-805.5
Exponent of deformation (rear) n_r	0.79	0.90	0.77	0.81
Cohesion c [kPa]	24.4	5.0	15.9	29.2
Angle of shear resistance φ [°]	18.0	30.0	25.6	6.4
Shear deformation modulus k [m]	0.014	0.010	0.010	0.012

Note. *C = Clay; CL = Clay loam; SL = Silty loam; LS = Loamy sand.

2.3 Tractor Properties and Traction Tests

A mechanical front wheel drive MFWD Hürlimann H488 DT tractor (Table 2) was used to perform traction tests. A second tractor, having weight higher than the pulling tractor, was used as braking machine (Figure 1). The tests were performed in steady-state motion along corridors of about 70 m, according to Battiato and Diserens (2013), considering four slip ranges: 5 ÷ 10%, 10 ÷ 15%, 15 ÷ 20% and 20 ÷ 30%. Two tractor configurations were considered by choosing tyre inflation pressures of 60 kPa and 160 kPa (Table 2).

A flat bed scale was employed to measure the wheel load in stationary condition. During the tests, a load cell measured the drawbar pull while a radar velocity sensor and a wheel speed sensor measured the actual forward velocity and the wheel rolling velocity, respectively. Details of the measuring instruments are given by Battiato and Diserens (2013). All the test parameters were recorded at a frequency of 1 Hz by a data acquisition system set on the braking machine (Figure 1). Outliers were eliminated and mean values were calculated for each range of slip.

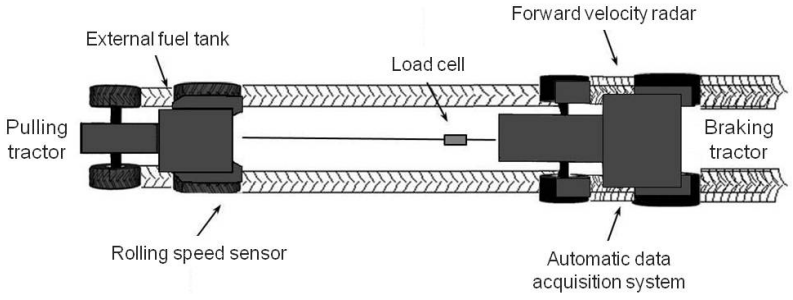

Figure 1. Layout of the tractor pulling test

The rolling radius of the tyres, in the considered configurations, was determined following indications of the ASAE Standard S296.2 (ASAE, 1983). According to Wismer and Luth (1973), the vehicle operating in self-propelled condition on a smooth road was assumed as reference condition (zero condition). The tyre slip was

calculated on the basis of the measured forward velocity, angular speed and rolling circumference.

During the tests, the fuel consumption was measured gravimetrically by using an external fuel can to fuel the tractor (Battiato & Diserens, 2013). The engine speed corresponding to the highest torque and the lowest specific fuel consumption of the engine (1700 rpm, 68% rated speed) was kept constant during the tests by means of the hand throttle. The tractor operated in the highest speed gear where power is not the limiting factor (Zoz, 1970). During the traction tests, the forward speed varied between 2.9 and 5.5 km/h, depending on the range of the slip.

Table 2. Tractor parameters

Tractor					Hürlimann H488 DT			
Power [kW]					65			
Weight [kN]					40			
Wheelbase L [m]					2.34			
Tyre (front-rear)					380/85R24-420/85R34			
Tyre width b (front-rear) [m]					0.38-0.44			
Tyre unloaded radius R (front-rear) [m]					0.63-0.79			
Rim diameter D_{rim} (front-rear) [m]					0.61-0.86			
Number of lugs (front-rear)					36-42			
Lug height (front-rear) [m]					0.026-0.034			
Tyre carcass stiffness K_{carc} (front-rear) [kN m^{-1}]					129.5-111.8			
Pressure dependence of tyre ΔK_p (front-rear) [kN m^{-1} kPa^{-1}]					1.22-2.00			
Configuration	1				2			
Height of the drawbar h [m]	0.80				0.83			
Stationary wheel load W_0 (front-rear) [kN]	9.1-10.9				9.1-10.9			
Tyre rolling radius R_r (front-rear) [m]	0.58-0.76				0.59-0.78			
Tyre inflation pressure P_{in} (front-rear) [kPa]	60-60				160-160			
Tyre stiffness (front-rear) [kN m^{-1}]	203-232				325-432			
	C*	CL	SL	LS	C*	CL	SL	LS
Soil-tyre contact area (front) [m^2]	0.20	0.18	0.19	0.19	0.17	0.16	0.16	0.15
Soil-tyre contact area (rear) [m^2]	0.24	0.24	0.26	0.25	0.20	0.18	0.21	0.19
Number of lugs on the contact area (front)	5.1	4.7	5.0	4.8	4.4	4.1	4.1	3.9
Number of lugs on the contact area (rear)	4.9	4.8	5.1	5.0	3.8	3.6	4.0	3.8

Note. *C = Clay; CL = Clay loam; SL = Silty loam; LS = Loamy sand.

2.4 Modelling of Traction Performance and Characterisation of Power Delivery Efficiency η_{PD} and Specific Fuel Consumption SFC

The traction performance of the 65 kW MFWD tractor was simulated with the tractor-soil interaction model introduced by Battiato and Diserens (2013). This model is based on the tyre-soil interaction model developed by Shmulevich and Osetinsky (2003) with the following assumptions: the soil behaves as a plastic non-linear medium; the wheel rolls at low velocity and in steady-state motion; the tyre deforms in linear elasticity; the tyre-soil contact surface has a parabolic form (with the apex at the rear point of contact) in the longitudinal direction; the wheel-soil interaction is two dimensional.

The tractor-soil interaction model (Battiato & Diserens, 2013) introduces: the multi-pass effect; the load transfer effect (dynamic wheel load); the relationship between the slip of the front wheel i_{front} and that of the rear wheel i_{rear} with rigid coupling between the front and the rear axles (theoretical speed ratio K_s). The values of K_s measured during preliminary tests in the configurations considered were very close to 1, (1.002 in configuration 1 and 0.997 in configuration 2), this allowed a simplified analysis based on the same slip value for the front and the rear wheel.

The traction performance was simulated in terms of drawbar pull DP, motion resistance MR, traction coefficient μ_{tr}, and traction efficiency η_{tr}. The drawbar pull DP, which represents the pulling force available at the tractor drawbar, was calculated as the sum of the net traction NT of the drive wheels:

$$DP = \sum NT \tag{1}$$

According to the model, the sum of the soil compaction resistance acting on the wheels R_c gives the motion

resistance of the tractor *MR*:

$$MR = \sum R_C \tag{2}$$

The drawbar pull *DP* to tractor weight $W_{tractor}$ ratio represents the traction coefficient μ_{tr}:

$$\mu_{tr} = DP / W_{tractor} \tag{3}$$

The fraction of power delivered to the tractor wheels and available as drawbar power is given by the traction efficiency η_{tr} of the tractor:

$$\eta_{tr} = DP\,V_a / \sum T\omega \tag{4}$$

where, T, V_a and ω are the total driving torque acting on the wheel, the actual forward velocity and the angular velocity of the wheel, respectively.

The parameters used for simulating the traction performance of the tractor in the two considered configurations are listed in Table 2.

For each simulation, the accuracy was assessed on the basis of the root mean square error RMSE:

$$RMSE = \sqrt{\frac{1}{n}\sum_{j=1}^{n}\left[Y(x_j) - \hat{Y}(x_j)\right]^2} \tag{5}$$

where, $Y(x_j)$, $\hat{Y}(x_j)$ and n represent the measured value, the corresponding predicted value and the number of samples in the validation set, respectively.

The ratio of the delivered tractive power to the input power from the tractor engine is described by the power delivery efficiency η_{PD} and represents the fraction of engine power available as tractive power (Shell, Zoz, & Turner, 1997; Turner, Shell, & Zoz, 1997).

According to Zoz, Turner, and Shell (2002), the equivalent power-take-off PTO can be used in order to consider the engine power input. In this case, the power delivery efficiency is given by:

$$\eta_{PD} = \frac{DP\,V_a}{Equivalent\ PTO\ power} \tag{6}$$

The equivalent *PTO* power was obtained on the basis of the measured fuel consumption, according to the experimental relationship between *PTO* and gravimetric fuel consumption (kg/h) at 1700 rpm, determined with a torque dynamometer and reported by Battiato and Diserens (2013).

Experimental points of η_{PD} at different slip i were fitted with the following equation (Battiato & Diserens, 2013):

$$\eta_{PD} = Ae^{\left(1-\frac{i}{l_A}\right)}\left(\frac{i}{l_A}\right)^{\left(1+\theta_A\frac{i}{l_A}\right)} \tag{7}$$

The ratio of the fuel consumption (gravimetric) to the drawbar power is defined as specific fuel consumption *SFC* (drawbar power basis). Experimental values of *SFC* at different slip i were fitted with the following equation (Battiato & Diserens, 2013):

$$SFC = \frac{1}{Be^{\left(1-\frac{i}{l_B}\right)}\left(\frac{i}{l_B}\right)^{\left(1+\theta_B\frac{i}{l_B}\right)}} \tag{8}$$

Fitting parameters A, l_A, θ_A of equation 7 and B, l_B, θ_B of equation 8 are defined according to Battiato and Diserens (2013).

3. Results and Discussion

3.1 Bevameter Tests

A comparison among the bevameter compression tests executed in the four sites (Figure 2) points out noticeable differences in the stiffness under compression of the four soils. Such differences persist both in the tests performed with the big plate as in the tests performed with the small plate. The loamy sand shows the highest stiffness, followed by the clay loam, whilst the silty loam and the clay are characterised by a lower stiffness. The clay soil shows the softest behaviour during the first load and the second load performed with the big plate (Figure 2*a*). In the compression tests with the small plate, the clay exhibits the weakest reaction during the first load and a reaction firmer than the silty loam during the second load (Figure 2*b*).

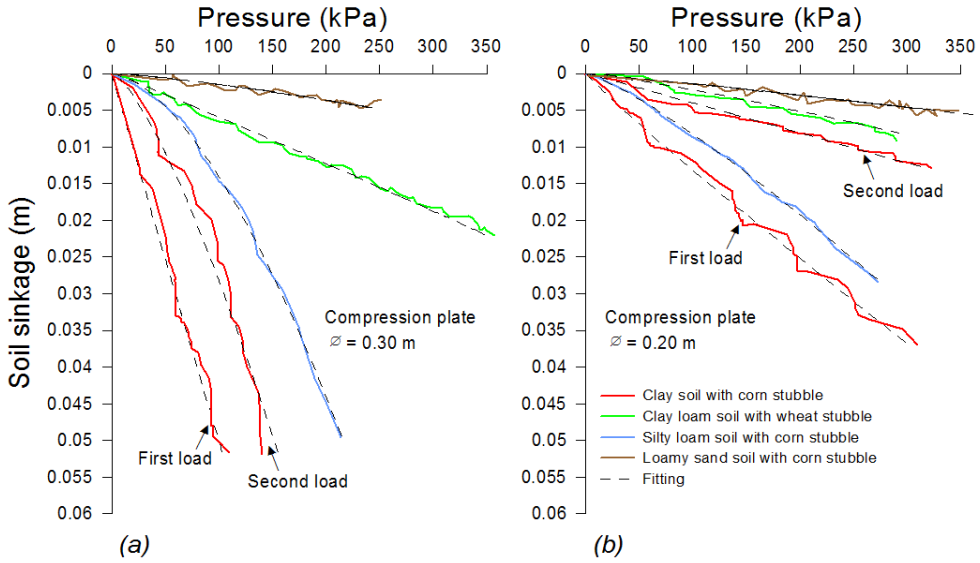

Figure 2. Bevameter compression curves with a round plate of diameter (*a*) 0.30 m and (*b*) 0.20 m

The Mohr-Coulomb envelopes of failure obtained for the four soils are reported in Figure 3. The loamy sand has the highest cohesion (c = 29.2 kPa) and the lowest angle of shear resistance (φ = 6.4°). This fact turns out in the highest strength at low vertical pressure and the lowest strength at high vertical pressure. An opposite mechanical behaviour is shown by the clay loam which has the lowest cohesion (c = 5 kPa) and the highest angle of shear resistance (φ = 30°). As a consequence, it has the lowest strength at low vertical pressure and the highest strength at high vertical pressure. The silty loam and the clay have values of cohesion and angle of shear resistance of 15.9 kPa and 25.6° and 24.4 kPa and 18°, respectively. In the range of vertical pressure lower than 22 kPa the loamy sand shows the highest strength, in the range of vertical pressure from 23 kPa to 55 kPa the highest strength is shown by the clay. In the range of vertical pressure above 56 kPa, the highest strength is that of the silty loam. The strength of the clay loam exceeds that of the silty loam at vertical pressures higher than 110 kPa.

The simulated mean normal stress and mean shear stress over the soil-tyre contact surface of the front and rear wheels at a slip of 10% and at a tyre pressure of 60 kPa and 160 kPa are reported in Figure 3 for the four soils under consideration. The mean normal stress under the rear wheel was higher than under the front wheel. The increase in tyre pressure made for a remarkable rise in mean normal stress and a minor increment in mean shear stress. The highest mean normal stress (68.4 kPa) and the highest mean shear stress (37.2 kPa) were reached on the loamy sand and on the silty loam, respectively, both at a tyre pressure of 160 kPa under the rear wheel.

The noticeable differences among the mechanical behaviour of the four soils under consideration are due to the variety of the soil textures and moisture conditions. Additional factors which affect, to a great extent, the soil mechanical response under tractor traffic-induced stress are the soil structure, the presence of a stubble cover and the previous stress state that the soil underwent.

Mechanical parameters of several soils obtained from compression and shear tests performed with a bevameter were reported by Wong (2008). An analysis of these results points out a rather wide variability of the soil parameters within the same texture of the soil, also for close values of the moisture content. Our tests highlight a high stiffness under compression, described by the parameters K_c, K_φ and n. Such a result depends on the fact that the soils under consideration were previously trafficked during the harvest. The cohesion of the loamy sand resulted quite high whilst the angle of shear resistance rather low. A possible reason for this result must be detected in the role of the stubble cover in affecting the shear resistance of the soil surface. The shear parameters measured on the other soils did not differ significantly from those reported by Wong (2008).

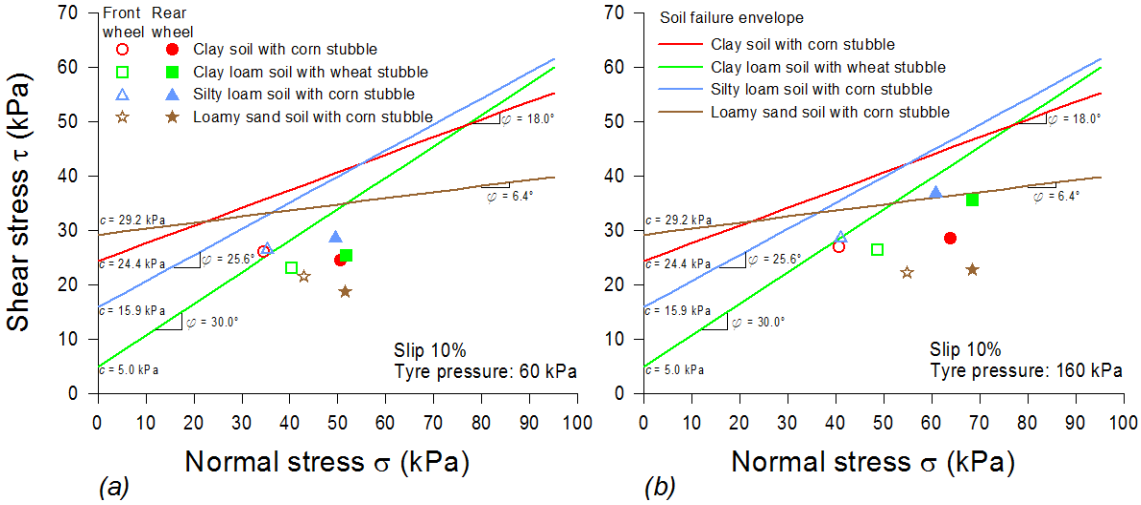

Figure 3. Soil failure envelopes and simulated mean normal and shear stress over the tyre-soil contact surface for the front and rear tractor wheels at a slip of 10% and tyre pressures of (*a*) 60 kPa and (*b*) 160 kPa

3.2 Measured and Simulated Drawbar Pull DP

Results of the traction tests carried out in the four sites are reported in Figure 4, in terms of drawbar pull-slip curve obtained in configuration 1 (Figure 4*a*) and in configuration 2 (Figure 4*b*). The experimental points are presented along with the simulations with the tractor-soil interaction model. The maximum measured drawbar pull DP_{max}, the corresponding slip and the root mean square error RMSE of the simulation are reported in Table 3.

Table 3. Maximum drawbar pull DP_{max}, corresponding slip and root mean square error RMSE of the simulation.

Tyre pressure	60 kPa				160 kPa			
Soil	DP_{max} kN	*Slip at* DP_{max}	*RMSE* kN	$RMSE_{overall}$ kN	DP_{max} kN	*Slip at* DP_{max}	*RMSE* kN	$RMSE_{overall}$ kN
Clay	28.5	28.0%	1.31	1.90	25.3	25.7%	1.62	1.70
Clay loam	25.6	27.2%	3.01		21.8	26.6%	2.90	
Silty loam	28.5	38.6%	2.14		25.9	46.7%	1.85	
Loamy sand	24.5	23.6%	1.14		18.9	26.6%	0.42	

At all the four sites, the increase in tyre pressure from 60 kPa to 160 kPa turned out in a decrease in drawbar pull. The overall variation from the lowest to the highest maximal drawbar pull measured on the four soils was about 16% at a tyre pressure of 60 kPa and 37% at a tyre pressure of 160 kPa.

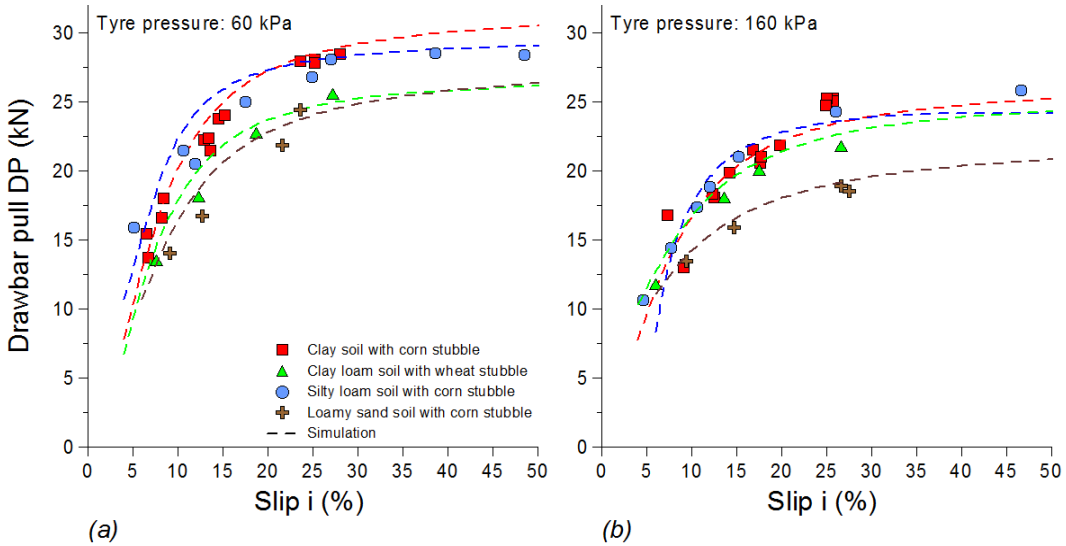

Figure 4. Measured and simulated drawbar pull *DP* on four soils at tyre pressures of (*a*) 60 kPa and (*b*) 160 kPa

Both the measured and the predicted drawbar pull pointed out the major role of the soil mechanical strength in controlling the traction performance of the used tractor. Particularly, the maximum drawbar pull that the tractor developed on the tested soils is a function of the available soil strength, according to the distribution of the normal stress over the soil-tyre contact surface (Figures 3*a* and 3*b*).

Considering a slip of 10%, which is a value inside the range where the power delivery efficiency is optimised and the specific fuel consumption is minimised (Figs. 8 and 9), the soil strength is expected not to be completely mobilised (Figures 3*a* and 3*b*). In this case, at a tyre pressure of 60 kPa, the simulated mean shear stress under the front and the rear wheels of the tractor was higher on the clay and on the silty loam than on the clay loam and on the loamy sand (Figure 3*a*). This fact turns out in a higher drawbar pull, both measured and simulated, on the clay and on the silty loam than on the clay loam and on the loamy sand (Figure 4*a*).

At a slip of 10% and a tyre pressure of 160 kPa, the simulated mean shear stress under the front and the rear wheels was noticeably higher on the silty loam than on the other soils. According to as above, also the measured and the simulated drawbar pull on the silty loam was higher than that on the other soils (Figure 4*b*). Moreover, in this case, the simulated mean shear stress on the loamy sand was remarkably lower than on the other soils (Figure 3) and similarly it was for the measured and simulated drawbar pull (Figure 4*b*).

Although the soil strength mainly controls the highest value of the drawbar pull, the way this latter varies with the slip depends on the geometry of the soil-tyre contact surface and on the rapidity with which the shear stress at the soil-tyre contact surface increases with the shear displacement. For soils with an elasto-plastic mechanical behaviour with hardening, like those under consideration and many other agricultural soils, such rapidity is characterised by the shear deformation modulus k. The higher the shear deformation modulus, the slower the shear stress increases with the shear displacement and the slower the drawbar pull increases with the slip, for a given soil-tyre contact surface. This fact explains why, at a low slip, the drawbar pull on the clay was lower than that on the silty loam, whilst, at a high slip, it resulted higher. The shear deformation modulus of the clay was 0.014 m, higher than that of the silty loam (0.010 m) and the highest among the soils considered (Table 1).

It must be observed that a higher mean normal stress over the soil-tyre contact surface makes for higher soil strength but, at the same time, increases the soil compaction resistance due to a deeper soil sinkage under the wheel. For a proper comparison among the stress states at the soil-tyre contact and the corresponding traction performance of the tractor in the cases presented, it should be considered that the soil-tyre contact surface depends, among factors such as the tyre geometry, the tyre stiffness and the wheel load, also on the soil stiffness during vertical compression. This latter is described by the cohesive (K_c) and the frictional (K_φ) modulus of deformation as well as by the exponent of deformation n (Table 1). These parameters were rather different among the considered soils and similarly it was for the soil-tyre contact surface (Tables 1 and 2).

In addition, it must be considered that the actual stress state over the soil-tyre contact surface is expected to be much more complex than that simulated by the used model as this latter does not properly describe the influence

of the tyre lugs on the stress state. Such aspect should be improved in the context of a further development of the model (Battiato & Diserens, 2017).

3.3 Simulations of Traction Coefficient μ_{tr}, Motion Resistance MR and Traction Efficiency η_{tr}

Results of the simulation with the tractor-soil interaction model at the four soils are reported in Figure 5, Figure 6 and Figure 7 in terms of traction coefficient μ_{tr}, motion resistance *MR* and traction efficiency η_{tr}, as a function of the slip in the range from 5% to 25% and as a function of the tyre pressure in the range from 60 kPa to 160 kPa.

On all the soils considered, the highest traction coefficient μ_{tr} was obtained at a tyre pressure of 60 kPa and a slip of 25% (Figure 5). The highest simulated traction coefficient was 0.69 on the clay. In the same conditions (tyre pressure of 60 kPa and slip of 25%), the highest traction coefficient on the clay loam, on the silty loam and on the loamy sand were 0.62, 0.68, and 0.60, respectively. In all the sites considered, the traction coefficient increased with the slip and decreased with the tyre pressure, at least for high values of slip.

Simulations of the traction coefficient μ_{tr} (Figure 5) on the four soils are in agreement with the measurements of the drawbar pull (Figure 4) and point out the major role of the soil strength parameters in controlling the development of traction. In particular, the soils which present the highest strength (soil failure envelope in Figure 3) within the range of normal stress of interest (30-70 kPa), like the clay and the silty loam, enable the development of the highest drawbar pull.

According to the used model (Battiato & Diserens, 2013), the soil strength is given by the sum of a cohesive component c and a frictional component $\sigma tan\varphi$, which depends on the normal stress σ. As a general rule, on soils whose shear strength is characterised by a high cohesive component, the highest improvements in the drawbar pull and traction coefficient are obtained with tractor configurations which imply a major increase in the soil-tyre contact surface (like a low tyre inflation pressure or the use of large wheels or dual wheels). On the contrary, on soils whose shear strength is largely controlled by the frictional component of resistance (high angle of shear resistance and low cohesion), significant improvements in drawbar pull are obtained by increasing the wheel load of the tractor. However, such improvements in drawbar pull might not correspond to improvements in traction coefficient (Battiato & Diserens, 2013, 2017).

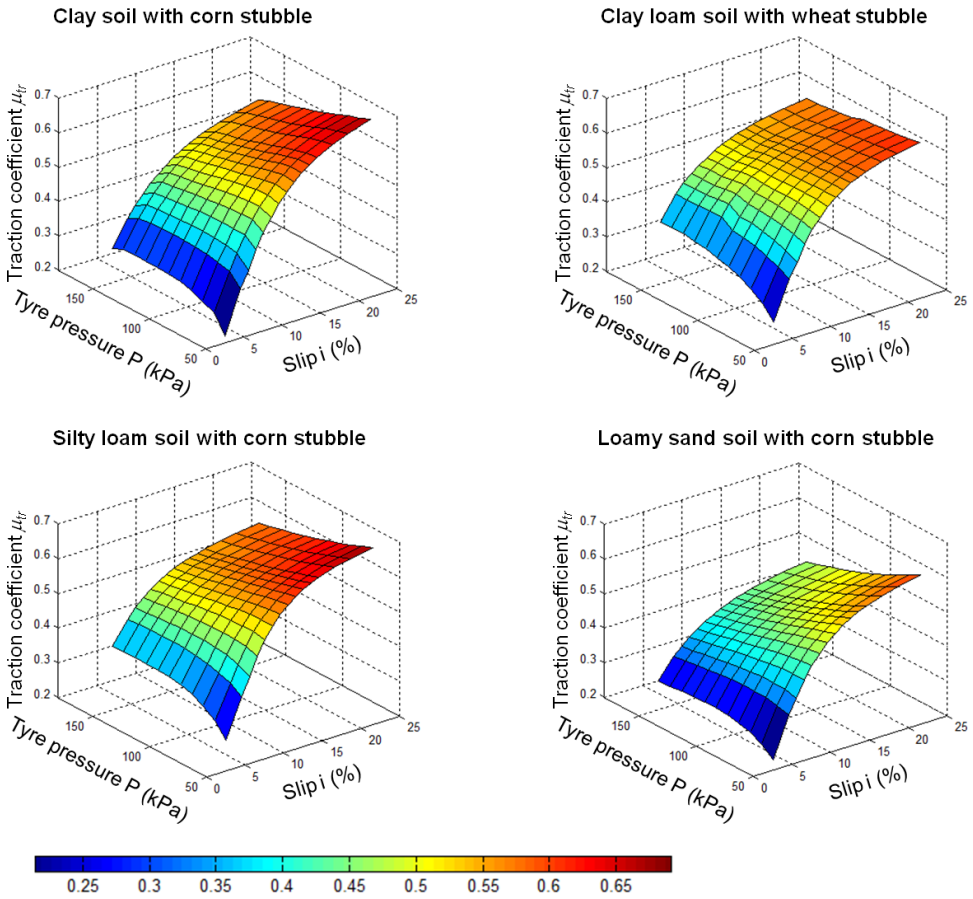

Figure 5. Simulation of the traction coefficient μ_{tr} of the Hürlimann H488 DT (65 kW) as a function of the slip and the tyre pressure on four different soils

In Figure 6, the motion resistance *MR* increased with the tyre pressure in all the cases considered. An increase in slip turned out in a reduction of motion resistance on the clay and in no significant variations on the other soils. The highest motion resistance was obtained on the silty loam at a tyre pressure of 160 kPa and a slip of 5%, and it was 2.17 kN. The highest motion resistance on the clay was 1.82 kN obtained at a slip of 5% and a tyre pressure of 160 kPa. On the clay loam, the maximum value of the motion resistance was 0.52 kN, obtained at a slip of 5% and a tyre pressure of 160 kPa. The maximum motion resistance on the loamy sand was 0.15 kN, obtained at a slip of 25% and at a tyre pressure of 160 kPa.

The comparison among the motion resistance simulated on the different soils is in agreement with the results of the compression tests reported in Figure 2. The motion resistance, calculated as the sum of the soil compaction resistances acting on the tractor wheels (Equation 2), represents the work performed by the tractor wheels in order to make ruts of a defined depth (Bekker, 1960) and depends on the soil stiffness under vertical compression. A high stiffness of the soil surface corresponds to a little rut depth and soil compaction resistance. An increase in tyre pressure makes for a smaller tyre-soil contact surface and a higher contact pressure which turns out in a deeper rut of the wheel and, as a consequence, in an increase in motion resistance. Due to the load transfer effect, the increase in slip produces a decrease in wheel load acting on the front wheel and a corresponding increase in wheel load on the rear wheel. This fact modifies the motion resistance more, like for the clay soil, or less substantially, like for the other soils.

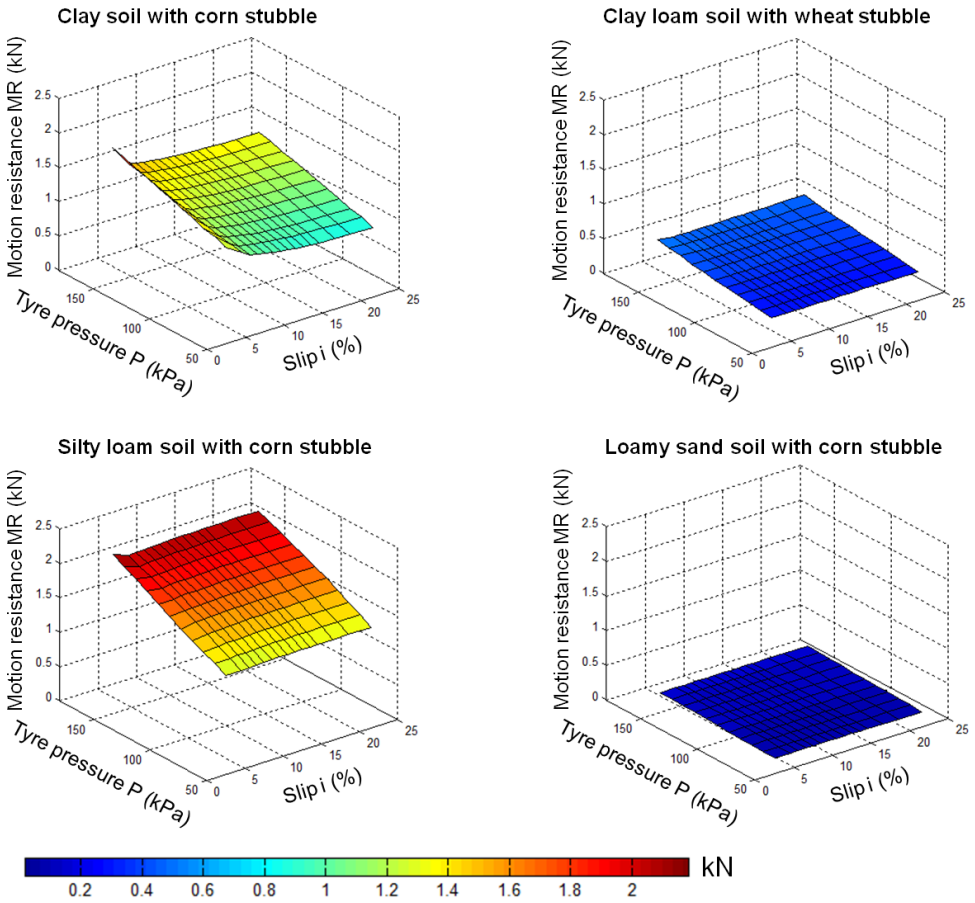

Figure 6. Simulation of the motion resistance *MR* of the Hürlimann H488 DT (65 kW) as a function of the slip and the tyre pressure on four different soils

The simulation of the traction efficiency η_{tr} in Figure 7 shows a peak in the range of slip values between 5% and 10%. The increase in tyre pressure makes mainly for a decrease in traction efficiency. The highest simulated traction efficiency was 0.95 reached on the loamy sand at a slip of 5%. The maximum traction efficiency on the clay, on the clay loam, and on the silty loam were, in order, 0.86, 0.92 and 0.85, reached at a slip of 10%, 5%, and 9%, respectively.

According to the elasto-plastic mechanical behaviour with hardening of the soils considered in this study, there is a first range of soil deformation within which the soil stress increases sharply, beyond this range the soil begins to deform considerably under a little increase in applied stress (Battiato, Diserens, Laloui, & Sartori, 2013). As a consequence, in the first range of soil deformation the drawbar pull increases substantially under a little increase in wheel slip, with increasing traction efficiency. Beyond this range, the drawbar pull increases slowly under a major increase in wheel slip, with a decrease in traction efficiency. Similar experimental distributions of the traction efficiency as a function of the slip or as a function of the drawbar pull have been reported by many authors since a long time (Davidson, Collins, & Mckibben, 1935; Wang, Kushwaha, & Zoerb, 1989; Zoz & Grisso, 2003).

The increase in tyre pressure turns out in a reduction in traction efficiency due to a reduced soil-tyre contact surface as well as a higher motion resistance (Battiato & Diserens, 2017).

The results of this study clearly show how the traction performance of a tractor is conditioned by the soil mechanical behaviour, being a characteristic of the tractor-soil system instead of the tractor only.

Similar results were recently reported by Pentoś and Pieczarka (2017) who observed that soil texture and moisture, both affecting, to a great extent, the mechanical response of the soil, had the highest influences on traction force and traction efficiency.

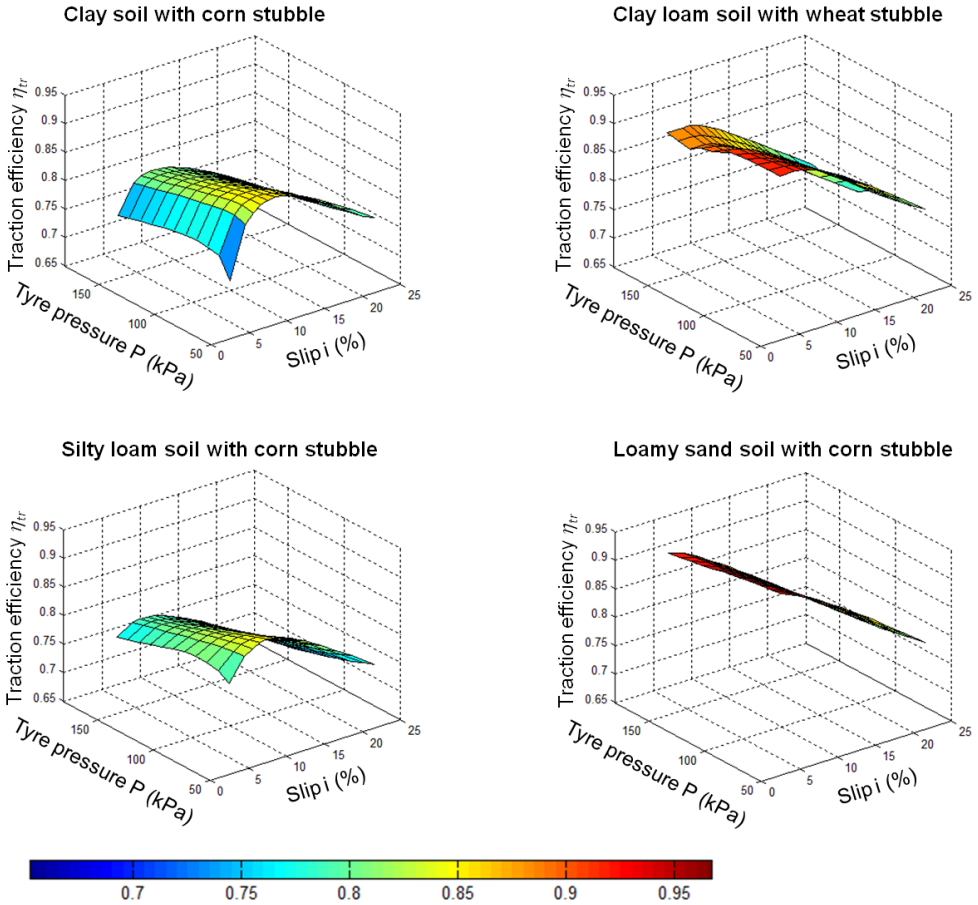

Figure 7. Simulation of the traction efficiency η_{tr} of the Hürlimann H488 DT (65 kW) as a function of the slip and the tyre pressure on four different soils

3.4 Measurement and Fitting of Power Delivery Efficiency η_{PD} and Specific Fuel Consumption SFC

In Figure 8 is reported the distribution of the power delivery efficiency η_{PD} as a function of the slip i, measured at a tyre pressure of 60 kPa (Figure 8*a*) and at a tyre pressure of 160 kPa (Figure 8*b*), at the four sites under consideration. Experimental points are seen along with a curve fitting based on Equation (7). Values of the maximum measured power delivery efficiency η_{PDmax}, the corresponding slip and the fitting parameters A, l_A, and θ_A (Equation 7) are reported in Table 4 together with the root mean square error RMSE.

Table 4. Maximum measured power delivery efficiency η_{PDmax}, corresponding slip, fitting parameters A, l_A, θ_A and root mean square error RMSE

Tyre pressure	60 kPa						160 kPa					
Soil	η_{PDmax}	*Slip at* η_{PDmax}	A -	l_A -	θ_A -	*RMSE* -	η_{PDmax}	*Slip at* η_{PDmax}	A -	l_A -	θ_A -	*RMSE* -
Clay	0.76	8.4%	0.67	3.77	0.28	0.019	0.65	16.8%	0.59	5.65	0.29	0.016
Clay loam	0.69	12.3%	0.65	0.07	0.27	0.008	0.66	13.6%	0.61	0.06	0.28	0.012
Silty loam	0.69	10.5%	0.67	0.04	0.27	0.057	0.65	15.2%	0.60	0.06	0.27	0.028
Loamy sand	0.64	9.1%	0.58	0.06	0.27	0.048	0.62	14.7%	0.58	0.06	0.28	0.008

The increase in tyre pressure from 60 kPa to 160 kPa turned out in an overall decrease in power delivery efficiency.

As for the distribution of the traction efficiency η_{tr}, also the distribution of the power delivery efficiency η_{PD} as a function of the slip is controlled by the elasto-plastic mechanical behaviour of the soil, accordingly, it presents an increasing phase followed by a decreasing one. Moreover, according to the reduction of traction efficiency with

the tyre pressure, also the power delivery efficiency decreases when tyre pressure increases. Similar distributions of the power delivery efficiency were reported by Zoz et al. (2002) as a function of the vehicle traction ratio.

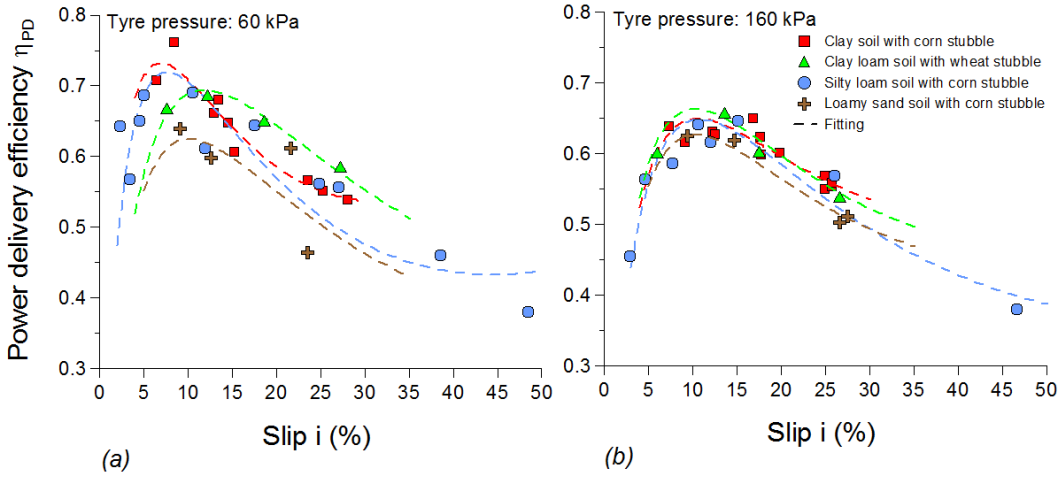

Figure 8. Measured and fitted power delivery efficiency η_{PD} on four different soils at a tyre pressure of (*a*) 60 kPa and (*b*) 160 kPa

Figure 9 reports the specific fuel consumption *SFC* [kg/kWh] (drawbar power basis) as a function of the slip *i*, measured at a tyre pressure of 60 kPa (Figure 9*a*) and at a tyre pressure of 160 kPa (Figure 9*b*), at the four soils under consideration. Measured points are seen along with a curve fitting based on Equation (8). The accuracy of the fitting was valued in terms of the root mean square error RMSE whose values are reported in Table 5 together with values of the fitting parameters B, l_B, and θ_B, the minimum measured specific fuel consumption SFC_{min} and the corresponding slip.

The distribution of the *SFC* shows a minimum in the range of slip from 7% to 15% both at a tyre pressure of 60 kPa and 160 kPa. The increase in tyre inflation pressure from 60 kPa to 160 kPa turned out in an overall increase in *SFC*.

Table 5. Minimum measured specific fuel consumption SFC_{min}, corresponding slip, fitting parameters B, l_B, θ_B and root mean square error RMSE

Tyre pressure	60 kPa						160 kPa					
Soil	SFC_{min} kg/kWh	*Slip at* SFC_{min}	B kWh/kg	l_B -	θ_B -	*RMSE* kg/kWh	SFC_{min} kg/kWh	*Slip at* SFC_{min}	B kWh/kg	l_B -	θ_B -	*RMSE* kg/kWh
Clay	0.32	8.4%	2.74	4.62	0.28	0.011	0.37	7.3%	2.47	5.26	0.29	0.010
Clay loam	0.35	12.3%	0.11	3.04	10.52	0.006	0.36	13.6%	0.11	2.99	11.02	0.004
Silty loam	0.37	10.5%	0.11	2.84	11.00	0.028	0.40	15.2%	0.09	3.04	10.52	0.018
Loamy sand	0.37	9.1%	0.10	2.50	10.50	0.029	0.38	14.7%	0.11	3.15	11.03	0.005

The distribution of the *SFC* as a function of the slip is strictly related to the distribution of the power delivery efficiency η_{PD} as an increase in power delivery efficiency mainly makes for a decrease in specific fuel consumption due to a better use of the soil strength as well as a reduction in the energy losses involved in the traction development and vice versa. Accordingly, the *SFC* increases with the tyre pressure.

Similar experimental results of the specific fuel consumption *SFC* were reported by Šmerda and Čupera (2010) as a function of the drawbar pull *DP*. According to our results, there is a narrow range of slip values inside which it is possible to minimise the specific fuel consumption of the tractor during tillage operations. Such a range (7-15% slip) did not vary significantly among the considered soils as well as with the tyre pressure (Figure 9), however, the *SFC* differed for almost 20% among the soils at a tyre pressure of 60 kPa and for ca. 10% at a tyre pressure of 160 kPa. Moreover, it rises up to 16% due to the increase in tyre pressure from 60 to 160 kPa. The slip range where the specific fuel consumption is minimised does not differ very much from the range where the

power delivery efficiency reaches a peak. The peak of power delivery efficiency varied noticeably, almost 20%, among the considered soils at a tyre pressure of 60 kPa and much less markedly, ca. 5%, at a tyre pressure of 160 kPa. It decreased up to 15% due to the rise in tyre pressure from 60 to 160 kPa. In conclusion, the different mechanical behaviour of the considered soils turned out to affect the fuel consumption and the power delivery efficiency more at low tyre inflation pressure than at high inflation pressure. Moreover, the increase in tyre pressure made for a decrease in power delivery efficiency and an increase in specific fuel consumption.

A proper match between tractor configuration and soil mechanical response, as well as an appropriate control of the wheel slip, may result in reduced costs of tillage operations due to the optimisation of the energy aspects involved in the traction development.

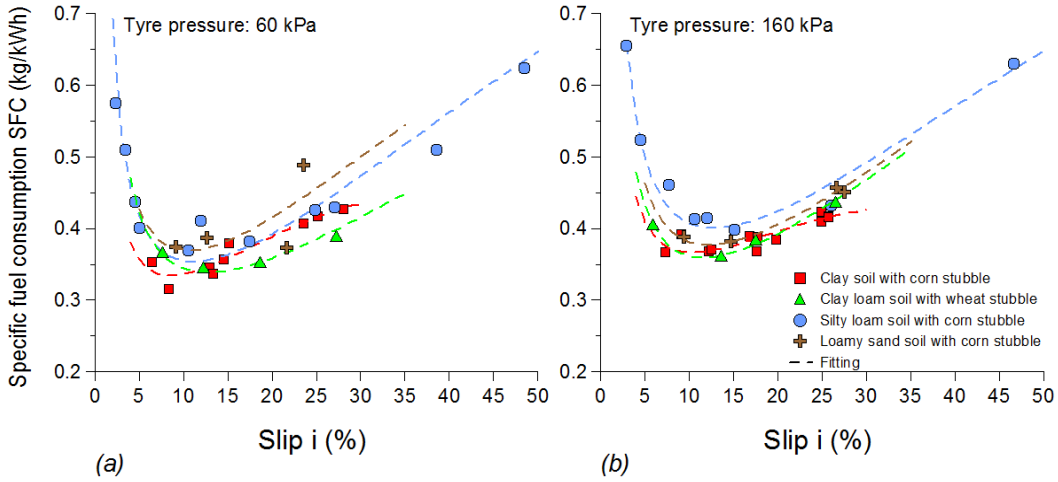

Figure 9. Measured and fitted specific fuel consumption *SFC* (drawbar power basis) on four different soils at a tyre pressure of *(a)* 60 kPa and *(b)* 160 kPa

4. Conclusions

The different mechanical behaviours of the four soils considered in this study affected the maximum drawbar pull of the 65 kW mechanical front wheel drive MFWD tractor used for the tests up to 16% at a tyre pressure of 60 kPa and 37% at a tyre pressure of 160 kPa.

The measured and simulated drawbar pull as well as the simulated traction coefficient, traction efficiency and motion resistance of the tractor on the four Swiss agricultural soils were in agreement with the mechanical response of the soils during compression and shear tests with a bevameter.

The presence of a cover of stubbles on the topsoil might affect the mechanical response of soil considerably. Therefore its role needs to be further investigated.

The specific fuel consumption (drawbar power basis) is minimised inside a narrow slip range which does not vary noticeably among the considered soils and with the tyre pressure. Moreover, it does not differ very much from the range where the power delivery efficiency reaches a peak. Differences in the specific fuel consumption of almost 20% at a tyre pressure of 60 kPa and about 10% at a tyre pressure of 160 kPa were observed among the considered soils. The increase in tyre pressure from 60 to 160 kPa makes for an increment in specific fuel consumption up to 16%.

The results of this study clearly pointed out how the optimisation of the energy aspects involved in the traction developed by a tractor depends, to a great extent, on the control of the wheel slip and on the choice of a tractor configuration which properly matches the mechanical response of the soil. This fact must be recognised of primary importance in developing strategies to reduce fossil fuel consumption and costs of tillage management as contribution to a sustainable crop production.

Acknowledgements

We wish to acknowledge Mr Jean-Pierre Clément and Mr Daniel Zürcher of the Swiss Federal Office for the Environment FOEN as well as Mr Gianni Covre and Mr Dominique Pittet of the Michelin for the valuable support to the project.

We also gratefully acknowledge the agricultural contractors who kindly put test sites and machineries at disposal for this work.

References

Battiato, A., & Diserens, E. (2013). Influence of tyre inflation pressure and wheel load on the traction performance of a 65 kW MFWD tractor on a cohesive soil. *Journal of Agricultural Science, 5*(8), 197-215. https://doi.org/10.5539/jas.v5n8p197

Battiato, A., Diserens, E., Laloui, L., & Sartori, L. (2013). A mechanistic approach to topsoil damage due to slip of tractor tyres. *Journal of Agricultural Science and Applications, 2*(3), 160-168.

Battiato, A., Diserens, E., & Sartori, L. (2014). Soil Compaction, Soil Shearing and Fuel Consumption: TASC V3.0 – A Practical Tool for Decision-Making in Farming. *Proceedings of the International Conference of Agricultural Engineering AgEng 2014, Zürich ETH, Switzerland, 6-10 July 2014, ref. C0528*.

Battiato, A., Alaoui, A., & Diserens, E. (2015). Impact of Normal and Shear Stresses Due to Wheel Slip on Hydrological Properties of an Agricultural Clay Loam: Experimental and New Computerized Approach. *Journal of Agricultural Science, 7*(4), 1-19. https://doi.org/10.5539/jas.v7n4p1

Battiato, A., & Diserens, E. (2017). Tractor traction performance simulation on differently textured soils and validation: A basic study to make traction and energy requirements accessible to the practice. *Soil and Tillage Research, 166*, 18-32. https://doi.org/10.1016/j.still.2016.09.005

Bekker, M. G. (1956). *Theory of Land Locomotion*. Ann Arbor, Mich., University of Michigan Press.

Bekker, M. G. (1960). *Off-the-Road Locomotion*. Ann Arbor, Mich., University of Michigan Press.

Burt, E. C., Bailey, A. C., Patterson, R. M., & Taylor, J. H. (1979). Combined effects of dynamic load and travel reduction on tire performance. *Trans. ASAE, 22*(1), 40-45. https://doi.org/10.13031/2013.34962

Burt, E. C., & Bailey, A. C. (1982). Load and inflation pressure effects on tires. *Trans. ASAE, 25*(4), 881-884. https://doi.org/10.13031/2013.33632

Charles, S. M. (1984). Effects of ballast and inflation pressure on tractor tire performance. *Agricultural Engineering, 65*(2), 11-13.

Damanauskas, V., Janulevičius, A., & Pupinis, G. (2015). Influence of Extra Weight and Tire Pressure on Fuel Consumption at Normal Tractor Slippage. *Journal of Agricultural Science, 7*(2), 55-67. https://doi.org/10.5539/jas.v7n2p55

Davidson, J. B., Collins, E. V., & Mckibben, E. G. (1935). Tractive Efficiency of the Farm Tractor. Agricultural experiment station Iowa state college of agriculture and mechanic arts. *Research Bulletin No. 189*. Ames, Iowa.

Diserens, E., & Steinmann, G. (2003). In-situ determination of the fracture point of an agricultural soil using the plate penetration test, comparison with the oedometer method and validation. *Proceedings of the International Conference on Geo-Environmental Engineering, Singapore* (pp. 93-106).

Diserens, E., & Battiato, A. (2013). *TASC V3.0—User Manual*. Agroscope.

Garciano, L. O., Upadhyaya, S. K., & Jones, R. A. (2010). Measurement of soil parameters useful in predicting tractive ability of off-road vehicles using an instrumented portable device. *J. Terramech., 47*(5), 295-305. https://doi.org/10.1016/j.jterra.2010.07.002

Lyasko, M. I. (2010). How to calculate the effect of soil conditions on tractive performance. *J. Terramech., 47*(6), 423-445. https://doi.org/10.1016/j.jterra.2010.04.003

Oenema, O., Heinen, M., Peipei, Y., Rietra, R., & Hessel, R. (2017). A review of soil-improving cropping systems. In E. Van den Elsen (Ed.), *Scientific report, project: Soil Care for profitable and sustainable crop production in Europe* (p. 59). Wageningen Environmental Research, The Netherlands.

Pentoś, K., & Pieczarka, K. (2017). Applying an artificial neural network approach to the analysis of tractive properties in changing soil conditions. *Soil Till. Res., 165*, 113-120. https://doi.org/10.1016/j.still.2016.08.005

Schreiber, M., & Kutzbach, H. D. (2008). Influence of soil and tire parameters on traction. *Res. Agr. Eng., 54*(2), 43-49.

Shell, L. R., Zoz, F. M., & Turner, R. L. (1997). Field performance of rubber belt and MFWD tractors in Texas

soils. *Belt and Tire Traction in Agricultural Vehicles (SP-1291)* (pp. 65-73). *SAE technical paper series 972729*. SAE. https://doi.org/10.4271/972729

Shmulevich, I., & Osetinsky, A. (2003). Traction performance of a pushed/pulled drive wheel. *J. Terramech., 40*, 35-50. https://doi.org/10.1016/j.jterra.2003.09.001

Šmerda, T., & Čupera, J. (2010). Tire inflation and its influence on drawbar characteristics and performance—Energetic indicators of a tractor set. *J. Terramech., 47*, 395-400. https://doi.org/10.1016/j.jterra.2010.02.005

Turner, R. J. (1993). A simple system for determining tractive performance in the field. *ASAE/CSAE meeting presentation, ASAE paper No. 93-1574*. St. Joseph, Mich.: ASAE.

Turner, R. J., Shell, L. R., & Zoz, F. M. (1997). Field performance of rubber belt and MFWD tractors in southern Alberta soils. *Belt and Tire Traction in Agricultural Vehicles (SP-1291)* (pp. 75-85). *SAE technical paper series 972730*. SAE. https://doi.org/10.4271/972730

Upadhyaya, S. K., & Wulfsohn, D. (1993). Traction prediction using soil parameters obtained with an instrumented analog device. *J. Terramech., 30*(2), 85-100. https://doi.org/10.1016/0022-4898(93)90022-P

Wang, G., Kushwaha, R. L., & Zoerb, G. C. (1989). Traction performance of a model 4WD tractor. *Canadian Agricultural Engineering, 31*(2), 125-129.

Wills, B. M. D. (1963). The measurement of soil shear strength and deformation moduli and a comparison of the actual and theoretical performance of a family of rigid tracks. *J. Agric. Eng. Res., 8*(2), 115-131.

Wong, J. Y. (1967). Behaviour of soil beneath rigid wheels. *J. Agric. Eng. Res., 12*(4), 257-269. https://doi.org/10.1016/S0021-8634(67)80044-1

Wong, J. Y., & Reece, A. R. (1967). Prediction of rigid wheel performance based on the analysis of soil-wheel stresses, part I. *J. Terramech., 4*(1), 81-98. https://doi.org/10.1016/0022-4898(67)90047-X

Wong, J. Y., & Reece, A. R. (1967). Prediction of rigid wheel performance based on the analysis of soil-wheel stresses, part II. *J. Terramech., 4*(2), 7-25. https://doi.org/10.1016/0022-4898(67)90047-X

Wong, J. Y., Garber, M., Radforth, J. R., & Dowell, J. T. (1979). Characterization of the mechanical properties of muskeg with special reference to vehicle mobility. *J. Terramech., 16*(4), 163-180. https://doi.org/10.1016/0022-4898(79)90026-0

Wong, J. Y. (1980). Data processing methodology in the characterization of the mechanical properties of terrain. *J. Terramech., 17*(1), 13-41. https://doi.org/10.1016/0022-4898(80)90014-2

Wong, J. Y., Radforth, J. R., & Preston-Thomas, J. (1982). Some further studies of the mechanical properties of muskeg in relation to vehicle mobility. *J. Terramech., 19*(2), 107-127. https://doi.org/10.1016/0022-4898(82)90015-5

Wong, J. Y., & Preston-Thomas, J. (1983). On the characterization of the shear stress-displacement relationship of terrain. *J. Terramech., 19*(4), 225-234. https://doi.org/10.1016/0022-4898(83)90028-9

Wong, J. Y. (2008). *Theory of Ground Vehicles*. John Wiley and Sons, Hoboken, New Jersey.

Zoz, F. M. (1970). Predicting tractor field performance. *ASAE paper No. 70-118*. St. Joseph, Mich.: ASAE. https://doi.org/10.13031/2013.37878

Zoz, F. M., Turner, R. J., & Shell, L. R. (2002). Power delivery efficiency: A valid measure of belt and tire tractor performance. *Trans. ASAE, 45*(3), 509-518. https://doi.org/10.13031/2013.8817

Zoz, F. M., & Grisso, R. D. (2003). Traction and tractor performance. *ASAE distinguished lecture series (Tractor design No. 27), ASAE publication No. 913C040*3. St. Joseph, Mich.: ASAE.

Notes

Note 1. The tractor-soil interaction model presented offered a valuable basis for the development of the application *TASC V3.0* for the practice. This is a useful tool which, in this third version, allows the user to assess and compare tractor traction performance, fuel consumption and soil vulnerability like severe risk of compaction or threshold of soil shearing due to slip, for different tractor and soil configurations.

For additional information, order or free usage of *TASC V3.0*, please contact Dr. E. Diserens: etienne.diserens@bluewin.ch

Copyrights

Copyright for this article is retained by the author(s), with first publication rights granted to the journal.

This is an open-access article distributed under the terms and conditions of the Creative Commons Attribution license (http://creativecommons.org/licenses/by/4.0/).